Supporting information

Light-triggered and Nanocarrier Properties of Nitrogen-doped Carbon Nanodots

Ludovica Maugeri,[a†] Grazia Maria Letizia Consoli,[b†] Giuseppe Forte,[a] Giorgia Fangano,[a] Loredana Ferreri,[b] Giuseppe Granata[b], Paolo Giuseppe Bonacci,[c,e] Nicolò Musso,[d,e] Luca Lanzanò[f], Elisa Longo[f], Marcello Marelli,[g] Angelo Ferlazzo[h], Antonino Gulino[h] and Salvatore Petralia[a,b,e]*

[a] *Department of Drug and Health Sciences, University of Catania, 95123 Catania, Italy*

[b] *CNR-Institute of Biomolecular Chemistry, 95126 Catania, Italy*

[c] *Department of Biomedical and Biotechnological Sciences, University of Catania, 95123 Catania, Italy*

[d] *Faculty of Medicine and Surgery, "Kore" University of Enna, Contrada Santa Panasia, 94100 Enna, Italy*

[e] *AIDA srl via S. Sofia, 97 Torre Biologica, 95123 Catania Italy*

[f] *Department of Physics and Astronomy "Ettore Majorana" University of Catania, 95123 Catania, Italy*

[g] *CNR-Institute of Science and Chemical Technologies "Giulio Natta", 20138 Milano, Italy*

[h]*Department of Chemical Sciences, University of Catania, 95123 Catania, Italy*

**corresponding author: Salvatore Petralia: e-mail: salvatore.petralia@unict.it*

Contents

Figure S10. Optical absorption spectra changes of CDs-chit/MB (1 mg ml^{-1}) water dispersion upon UV-light irradiation in deaerated condition.

Figure S11. Optical absorption spectra changes of CDs-chit/MB (1 mg ml^{-1}) water dispersion upon UV-light irradiation in dark condition.

Figure S12. Absorption spectra of the aggregate 1-a at CAM-B3LYP/6-311+G(d,p)/CPCM level.

Figure S13. Representation of the simulated model in water solvent; curcumin is represented in yellow, chitosan in grey.

Figure S14. Stability test: Absorbance@350nm for Cds-chit in water over time: 0.5, 1, 3 and 6 months.

Figure S15. Optical spectra spectra of Cds-chit/curc in PBS at 0 and 6 months form the preparation.

Table S1. Biophotometer and Qubit quantification related to RNA extraction.

Table S2. Supported Combinations provided for the generation of the Illumina protocol followed for the preparation of the libraries.

Table S3. Fold change data calculated for HCT-116 cell line treated with CDs-chit.

Table S4. Fold change data calculated for HeLa-116 cell line treated with CDs-chit.

Table S5. XPS peaks assignment.

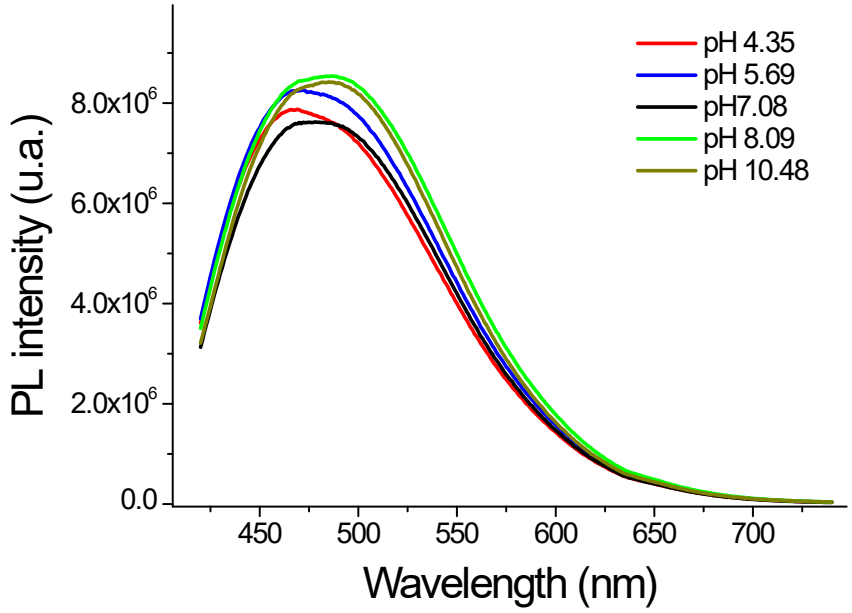

Figure S1. Emission spectra of CDs-chit nanostructures in water at different pH: 4.35, 5.7, 7.08, 8.39 and 10.5 ($\lambda_{exc.}$=400 nm, Abs_{400nm}= 0.13, slits 2/2 mm)

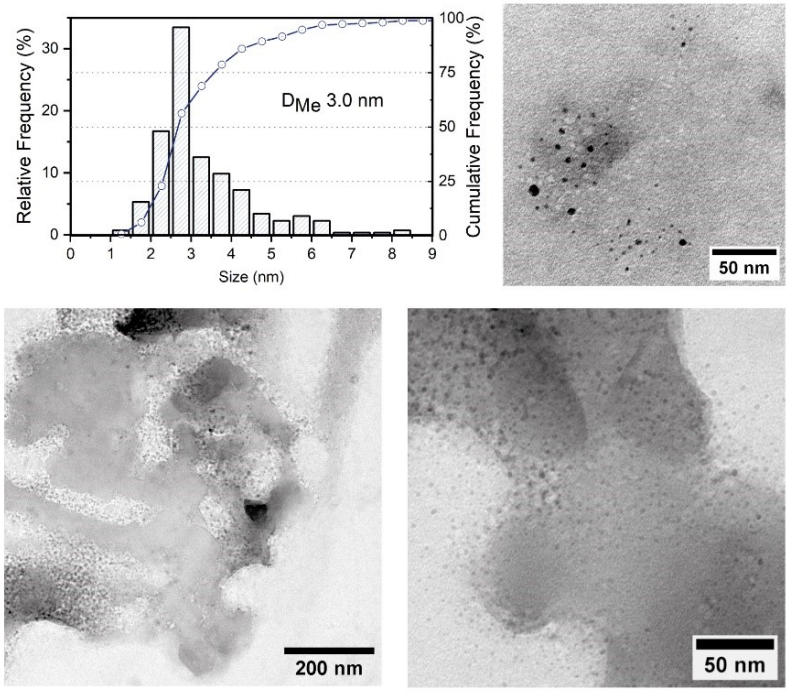

Figure S2. Size Distribution Graph and representative TEM micrographs for CDs-chit nanostructures. Spherical nanoparticles appear relatively homogeneous in size without agglomerates or oversized nanoparticles.

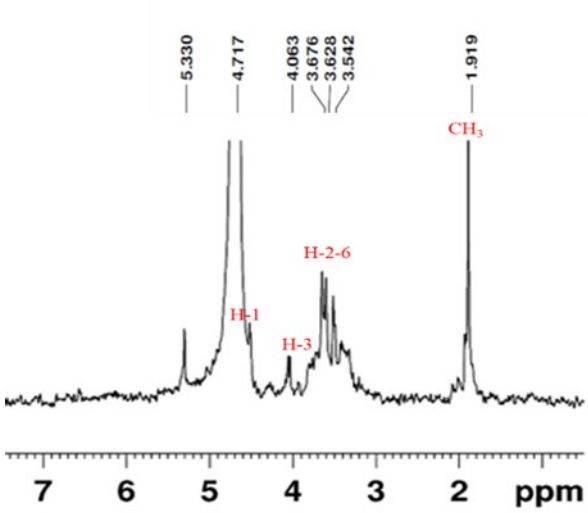

Figure S3. ^{1}H-NMR spectrum of Cdots-chit (400.13 MHz, D_2O, 297 K).

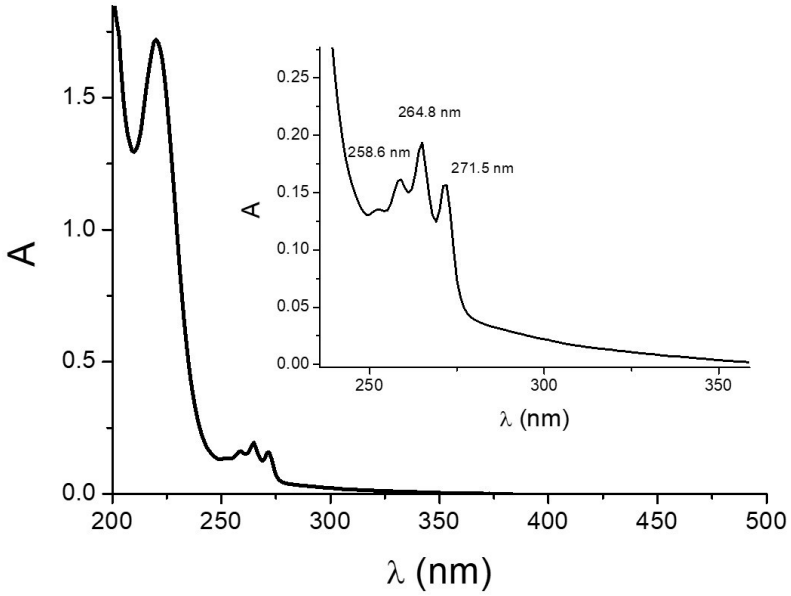

Figure S4. Optical absorption spectra of the CDs prepared at 400 °C for 4 hrs in air and dissolved in water (pH 7.2). Experiments, performed at high 400 °C for 4 hrs) exhibits the formation of CDs with typical optical absorption spectrum of polyaromatic structures (Figure S1). Moreover, the lower water dispersibility of this fully carbonized nanostructures agreed with the complete carbonization of chitosan to form CDs core.

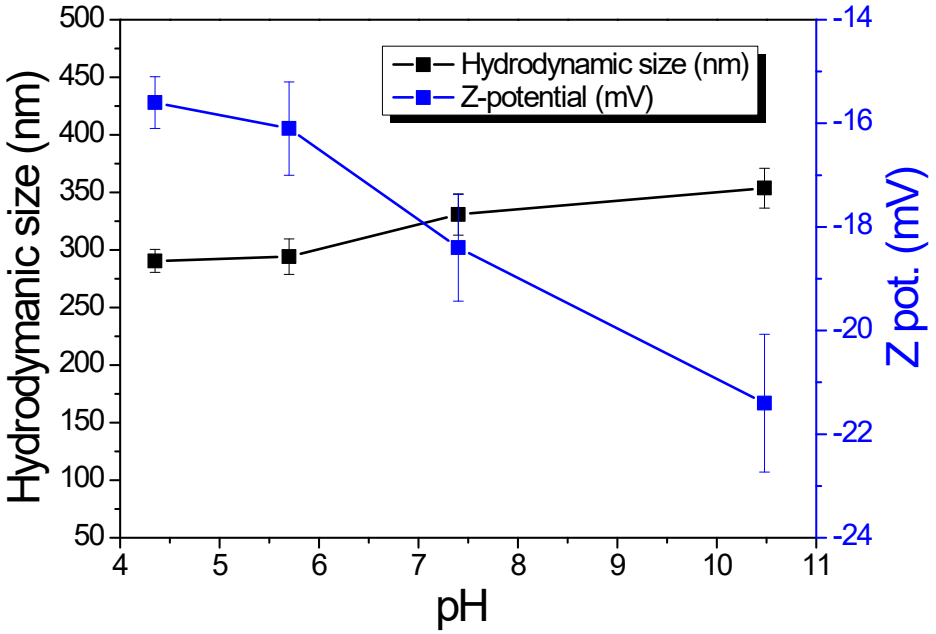

Figure S5. Hydrodynamic diameter and Z-potential measurements of CDs-chit (1 mg mL^{-1}) in water at different pH values.

Photothermal conversion efficiency (η)

Photothermal measurements were performed irradiating a volume of 100 µL of CDs-chit dispersion for 10 minutes in a glass tube (diameter 3 mm), using continuous wave Laser at different laser power and at different wavelength excitation (405 and 808 nm). A standard infrared thermal imaging camera was used to measure the temperature of the solution every 20 seconds, during the heating and cooling processes. The photothermal conversion efficiency (η) was calculated according to equation (1) introduced by Roper

$$\eta = \frac{hA\,(T_{max} - T_{surr}) - Q_{Dis}}{I(1 - 10^{-A})} \quad (1)$$

Where T_{max} and T_{surr} represents the max photothermal temperature and the ambient temperature respectively, I is the incident laser power and A is the absorbance value of CDs-chit dispersion at the wavelength excitation. The equations (2) and (3) were introduced to calculate the parameter hA.

$$\theta = \frac{T - T_{surr}}{T_{max} - T_{surr}} \quad (2)$$

$$\tau = \frac{M_D\, C_D}{hA} \quad (3)$$

where MD and CD are the mass (0.1 g) and heat capacity (4.2 J g^{-1}) of water respectively, and τs is the time constant, calculated by the equation (4).

$$t = -\tau(ln\theta) \quad (4)$$

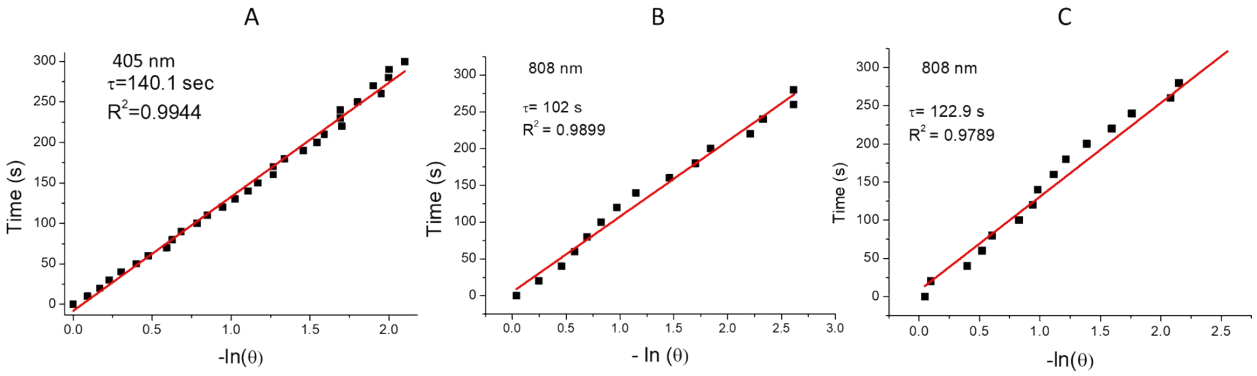

Figure S6. Linear relationship between time (sec) and -ln(θ), the slope is the time constant (τ_s) for photothermal experiments of: A) CDs-chit sample (Ass= 4.5) upon excitation with laser wavelength 405 nm (power 211 mW), B) CDs-chit sample (3.3 mg mL-1) upon excitation with laser wavelength 808 nm (1 W) and C) CDs-chit sample (6.6 mg mL-1) upon excitation with laser wavelength 808 nm (1 W).

Photochemical preparation of CDs-chit/Au nanostructures

The formation of CDs-chit/Au nanostructures at different concentrations of $HAuCl_4$ precursor (5.6×10^{-5} M, 1.6×10^{-4} M, and 4.8×10^{-4} M), after degassing with argon (15 min), was observed at different irradiation times using two UV lamps operating at 300 nm as well as assessments conducted under dark conditions. The same experiment was performed for the chitosan precursor (1 mg/ml

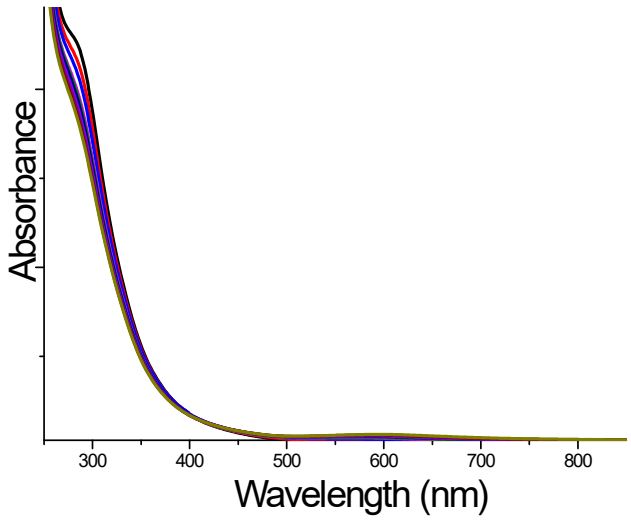

precursor and 1.6×10^{-4} M $HAuCl_4$).

Figure S7. Dark control experiment: Optical absorption spectra of Au-nanostructures formation using 0.53 mM $HAuCl_4$ in water and CDs-chit (1 mg mL^{-1}), without light, at different time from 0 to 120 min.

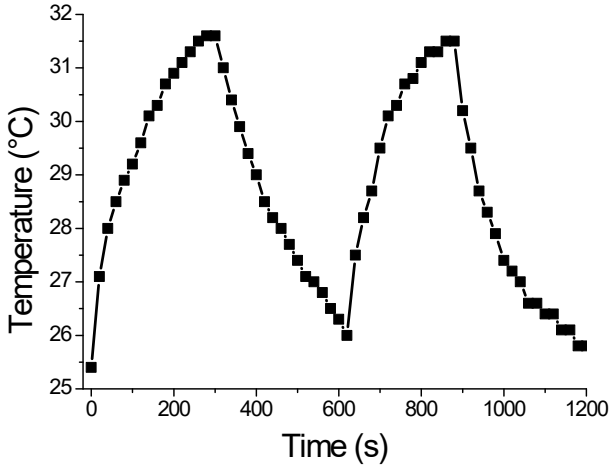

Figure S8. CDs-chit/Au photothermal experiments: photothermal cycles (laser 532 nm, laser power 200mW)

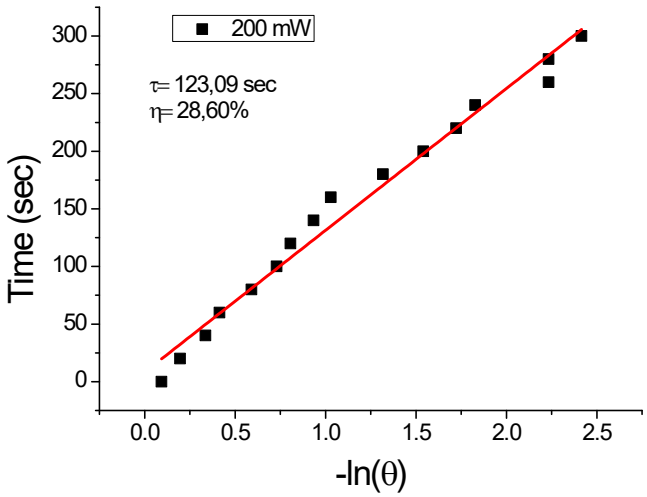

Figure S9. CDs-chit/Au photothermal experiments: Linear relationship between time (s) and -ln(θ), the slope is the time constant (τ_s) for photothermal experiments at laser wavelength 532 nm and laser power 200 mW.

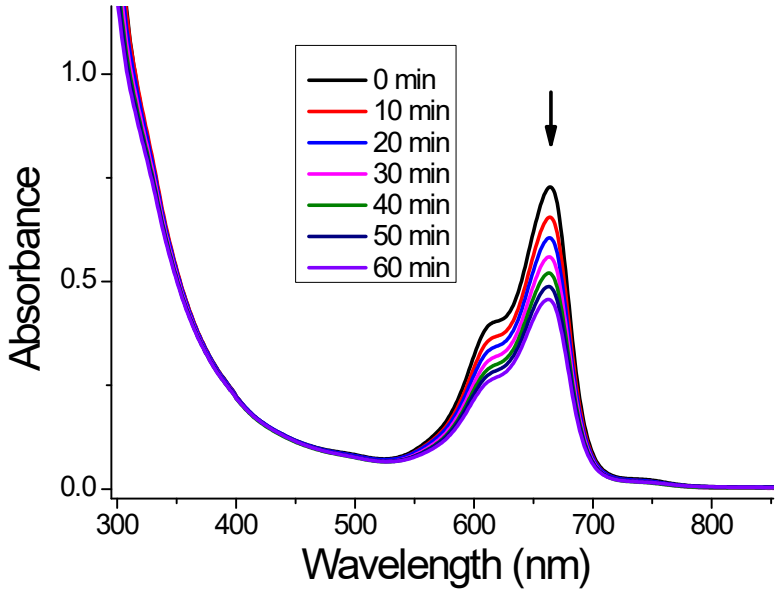

Figure S10. Optical absorption spectra changes of CDs-chit/MB (1 mg ml^{-1}) water dispersion upon UV-light irradiation (10, 20, 30, 40, 50 and 60 min, 2 lamps 300 nm) in aerated condition.

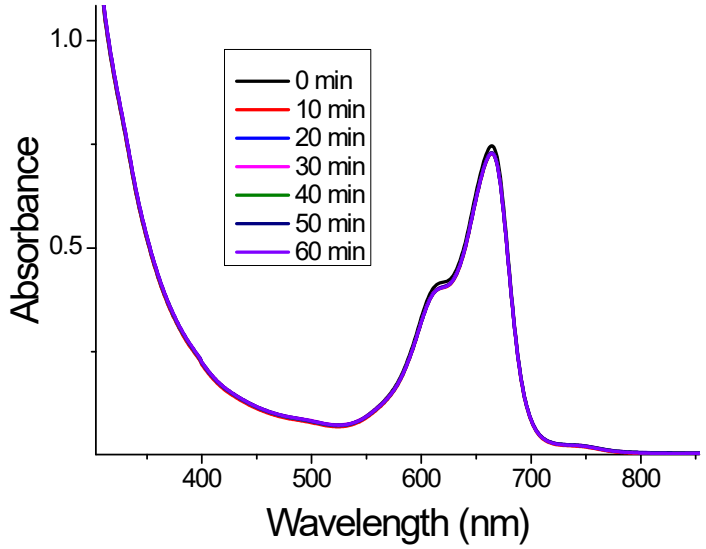

Figure S11. Optical absorption spectra changes of CDs-chit/MB (1 mg ml^{-1}) water dispersion upon UV-light irradiation (10, 20, 30, 40, 50 and 60 min,) in dark condition.

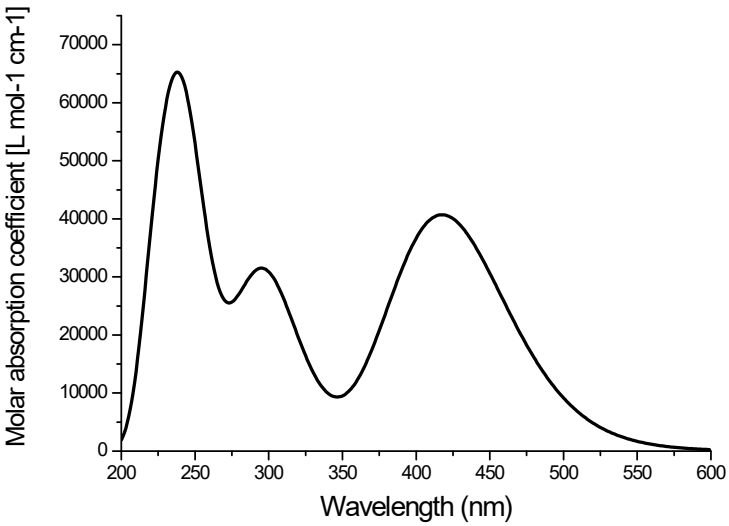

Figure S12. Absorption spectra of the aggregate 1-a at CAM-B3LYP/6-311+G(d,p)/CPCM level.

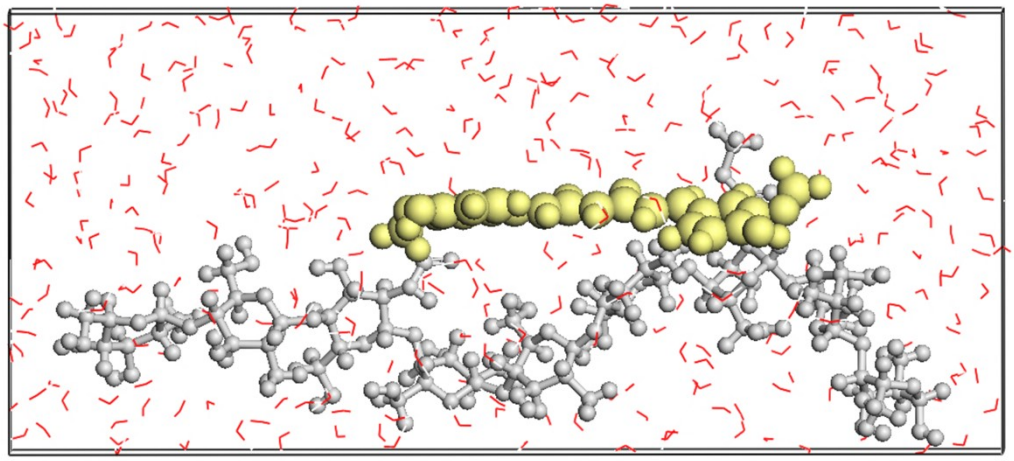

Figure S13. Representation of the simulated model in water solvent; curcumin is represented in yellow, chitosan in grey.

RNAseq Experiment

HeLa and HCT 116 cells were plated in a 6-well plate (Cat. No. 30006, SPL Life Sciences Co., Ltd. 48, Geumgang-ro 2047 beon-gil, Naechon-Myeon, Pocheon-si, Gyeonggi-do 487 835, Korea) at a concentration of 100.000 cell per well and after 24 hours, they were treated for 6 hours with a concentration of CDs-Chit/Cur nanoparticles equal to 40 ng μL^{-1}, that in a working volume of 500 µL corresponds to 20 µg per well. Each treatment was carried out in triplicate. Untreated cells were used as a control. After six hours, cells supernatant was removed and cells were resuspended in 300 µL of RLT Buffer (Cat. 74104, Qiagen, Hilden, Germany) with a concentration of β- mercaptoethanol (Cat. M6250, Merck, 126 East Lincoln Avenue P.O. Box 2000. Rahway 07065, United States) equal to 10 µL mL^{-1} and in 300 µL of 70% ethanol. The cells were finally frozen at -80 °C awaiting RNA extraction.

RNA extraction and quantification

The RNA has been extracted following the manufacturer's instructions of the Qiamp RNeasy Mini Kit (Cat. 74104, Qiagen, Hilden, Germany); the integrity and the quantification of the RNA were attest using Agilent RNA 6000 Nano Kit (Cat. 5067-1511, Agilent, Santa Clara, CA 95051, USA) on a 2100 Bioanalyzer Instrument (Cat. G2939BA, Agilent, Santa Clara, CA 95051, USA) and also using Qubit™ RNA HS Assay Kit (Cat. 2390601, Invitrogen, Eugene, Oregon, USA) on a Qubit 4 Fluorometer instrument (Cat. Q33238, Invitrogen, Eugene, Oregon, USA). The samples and their quantifications are given in Table x.

Table S1. Biophotometer and Qubit quantification related to RNA extraction. Qubit quantification is expressed as average of triplicate.

Number	Sample	Biophotometer Quantification (ng/µL)	Qubit Quantification (Average, ng/µL)
1	HeLa Untreated	72.1	87.8
2		69.3	
3		77.2	
4	Hela Treated	50.5	69.3
5		79.4	
6		89.6	
7	HCT-116 Untreated	80.3	77.3
8		57.63	
9		45.4	
10	HCT-116 Treated	50.8	45.8
11		84.1	
12		75.2	

Table S2. Supported Combinations provided for the generation of the Illumina protocol followed for the preparation of the libraries.

Sequencing Instrument	MiSeq
Library Preparation Kit	AmpliSeq for Illumina Custom and Community Panels
Input Material	Only RNA protocol
Indexing	Dual Indexing
Reagent Kits	MiSeq Reagent Kit v3

Table S3. Fold change data calculated for HCT-116 cell line treated with CDs-chit.

HCT-116	Max group mean	Log_2 fold change	Fold change	P-value
ABCC1	720.68	0.22	1.17	0.49
ABCC2	3,643.47	0.23	1.17	0.59
BAX	3,202.63	-0.46	-1.38	0.32
BCL2	30.13	-0.62	-1.54	0.39
CAT	3,366.31	-0.31	-1.24	0.45
CCL5	4.51	2.01	4.03	0.3
CHRNA2	1.42	3.36	10.27	0.14
CHRNB2	0.56	-2.9	-7.44	0.52
GCLC	8,310.76	0.5	1.42	0.02
GCLM	4,498.82	0.41	1.33	0.4
GPX1	54,335.49	-0.52	-1.43	0.26
GSTP1	47,663.06	0.01	1.01	0.96
HMBS	1,854.51	-0.13	-1.1	0.75
HMOX1	5,024.49	-0.2	-1.15	0.63
IDE	4,074.58	0.11	1.08	0.67
IL10	1,24	-2.55	-5.84	0,58
IL1B	512,33	-9.34	-647.15	0,07
IL1RN	37.19	0.88	1.85	0.28
IL6	994.56	-6.18	-72.28	0.01
IL8	2.647.18	-1.21	-2.31	0.14
JUN	4.43	-1.49	-2.81	0.34
KCNK13	461.69	-0.32	-1.25	0.15
KEAP1	3,168.35	0.05	1.04	0.88
LRP1	129.83	-0.18	-1.13	0.6
MMP2	5.27	1.33	2.51	0.54
MMP9	1.75	-3.18	-9.04	0.48
MRPL13	313.38	0.02	1.02	0.97
NFE2L2	6,157.34	0.82	1.76	0.06
NFKB1	2,071.30	0.27	1.2	0.53
NQO1	21,709.60	0.28	1.21	0.51

PARK7	31,854.19	-0.6	-12	0.31
PRDX1	2,066.81	0.08	1.05	0.8
PRDX3	39,553.13	-0.02	-1.01	0.95
PTGS2	293.37	-0.1	-1.07	0.89
SOD1	77,329.17	-0.18	-1.13	0.61
SOD2	2,827.36	-0.16	-1.12	0.41
SRXN1	2,925.22	0.28	1.21	0.59
TGFB1	6,000.67	-0.23	-1.17	0.45
TGFBR2	378.68	0.18	1.14	0.84
TNF	0.49	-1.4	-2.64	0.76
TXN	58,116.93	-0.16	-1.12	0.35
TXN2	19,196.80	-0.05	-1.03	0.81
TXNRD1	35.7	0.12	1.09	0.93
VEGFB	4,778.08	-0.17	-1.13	0.65

Table S4. Fold change data calculated for HeLa-116 cell line treated with CDs-chit.

HeLa	Max group mean	Log_2 fold change	Fold change	P-value
ABCC1	86.74	0,25	1.19	0.77
ABCC2	62.63	-0.78	-1.71	0.54
BAX	1,563.70	-0.19	-1.14	0.59
CAT	1,960.56	0.13	1.1	0.84
CCL2	311.82	0.7	1.63	0.69
CCL5	13.27	-1.83	-3.56	0.48
GCLC	1,745.62	0.49	1.41	0.6
GCLM	4,123.44	0.22	1.16	0.79
GPX1	80,271.05	0.6	1.51	0.59
GSTP1	5,428.89	0.51	1.42	0.68
HMBS	5,751.07	-0.01	-1.01	0.98
HMOX1	24,241.53	0.66	1.58	0.52
IDE	2,990.18	0.43	1.35	0.34
IL1B	26.96	1.92	3.79	0.53
IL6	2,281.86	-0.28	-1.21	0.83
IL8	3,115.79	-0.57	-1.49	0.73
JUN	34.6	0.75	1.68	0.7
KEAP1	613.93	0.2	1.15	0.78
LRP1	824.08	0.28	1.21	0.71
MMP2	941.69	0.13	1.09	0.65
NFE2L2	2,130.13	0.24	1.18	0.83
NFKB1	424.7	0.17	1.13	0.73
NQO1	19,618.07	0.64	1.56	0.62
PARK7	47,941.35	1.05	2.07	0.32
PRDX1	4,924.10	0.13	1.1	0.77
PRDX3	24,352.09	0.8	1.75	0.46
PTGS2	501.22	0.31	1.24	0.63
SOD1	51,714.48	0.66	1.58	0.59
SOD2	2,539.99	0.75	1.68	0.39
SRXN1	1,773.15	-0.09	-1.07	0.88

TGFB1	13,505.91	0.65	1.57	0.51
TGFBR2	80.51	-0.33	-1.25	0.8
TNF	10.93	1.92	3.79	0.48
TXN	55,142.76	0.4	1.32	0.72
TXN2	12,413.53	0.41	1.33	0.68
VEGFB	22,097.49	0.67	1.59	0.42

Table S5. XPS peaks assignment.

Species	**chitosan**	**CDs_chitosan**	**assignment**
C 1s	----	284.3	sp^2
	285.0	285.0	sp^3 C-C, C-H
	285.5	285.5	C-N
	286.5	286.4	C-OH
	288.1	288.2	O-C-O, C=O
O 1s	531.1	531.5	C=O
	532.7	532.5	C-O
		533.9	H_2O
N 1s	399.3	399.6	-NH_2, C-N-C,
	400.3	400.6	N-C=O
	401.6	401.9	N^+, graphitic N

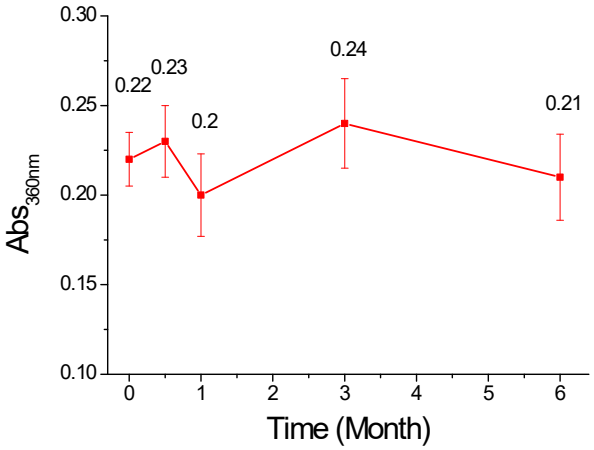

Figure S14. Stability test: Absorbance@350nm for Cds-chit in water over time: 0.5, 1, 3 and 6 months.

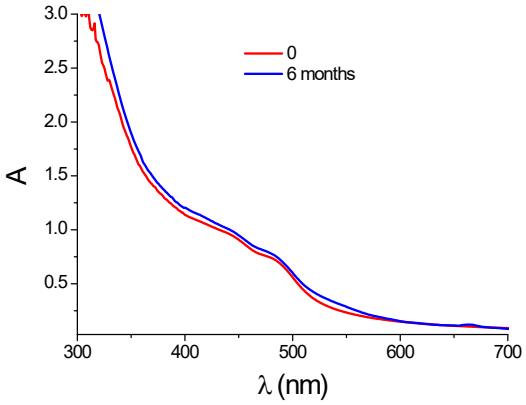

Figure S15. Optical spectra spectra of Cds-chit/curc in PBS at 0 and 6 months form the preparation.